Propagative slipping modes in a spring-block model

Pep Español
Cavendish Laboratory, Cambridge University, Madingley Road CB3 OHE, United Kingdom and Departamento de Física Fundamental, Universidad Nacional de Educación a Distancia, Apartado 60141, 28080 Madrid, Spain
(Received 5 November 1993)

Two transitions are observed in a version of the Burridge-Knopoff model of a tectonic fault. The first transition has already been reported and occurs when the velocity scale of the friction force is varied. We trace the origin of this transition back to what is happening for a single free block. The second transition is observed when varying the speed of sound of the system and concerns the possibility that the system exhibits solitary wave solutions. We provide a necessary condition for the system having a stable solitary wave solution. This condition, which involves a single parameter formed with three of the four parameters of the system, allows one to interpret some of the numerical results.

PACS number(s): 64.60.Cn, 83.50.Tq, 91.30.−f

I. INTRODUCTION

In order to understand the ubiquitous presence of fractal structures in nature, Bak, Tang, and Wiesenfeld [1] introduced in 1987 the concept of self-organized criticality. This appealing idea has stimulated since then a large number of studies of systems as different as sand piles [1], water erosion [2], and network rivers [3], or earthquakes [4]. In the case of earthquakes, the Gutenberg-Richter law implies a power law for the probability distribution of seismic moments of events and it has been regarded as an indication that the brittle fracture in the tectonic fault critically self-organizes the fault. For this reason, much effort has been devoted to the design of simple models which capture the relevant features of a tectonic fault and, in particular, produce a power law distribution of seismic moments.

A simple model which accomplishes this is a deterministic homogeneous one-dimensional (1D) version of the Burridge and Knopoff model [5]. This model has received much attention recently [6–10]. Carlson and Langer identify three types of events: (1) Microscopic events involving only a few blocks with maximum velocities less than the pulling speed; these events tend to smooth the inhomogeneities in the system, (2) localized events with velocities larger than the pulling speed (some stress is relaxed with these events), and (3) delocalized events whose velocities are much larger than the localized events and release efficiently the majority of the stress [6]. It is observed numerically that the delocalized events are accompanied by fractures which propagate at the order of the speed of sound. The selection mechanism of the speed of the cracks has been studied analytically by Langer and Tang [8]. A recent observation on the same model is that at higher energy input rates the fractures span the entire system and, for periodic boundary conditions, solitary wave solutions appear [10]. These propagating macrodislocations are specially relevant in a recent laboratory experiment on earthquakes [11]. In this experiment, Rubio and Galeano place an elastic gel between two corotating cylinders and they measure with a photoelastic technique the relaxation of the stress due to slip with the boundary. They also describe two types of characteristic motion depending on the rotational velocity of the inner cylinder. For small rotational velocities they observe small localized slip events (but with exponential statistics) and for large rotational velocities they observe propagating slipping regions.

Another system where there appears a transition from chaotic-type to solitary-wave-type solutions is in the extrusion of a highly viscoelastic polymer melt through a die [12]. Two surface defects are usually observed in the extrudate which are termed sharkskin and helicoidal fracture, respectively. Sharkskin is a small amplitude surface defect that appears above a certain critical pressure of extrusion. At even higher pressures the extrudate exhibits helicoidal patterns [13]. We suggest that the dynamics of the stress relaxation at the die exit responsible for sharkskin and helicoidal patterns is essentially the same as that of a tectonic fault [14]. In this way, slipping regions may be localized, giving rise to sharkskin, or propagate along the lip of the die exit, producing the helicoidal pattern observed.

It seems that the comprehension of the way solitary waves arise in spring-block models is important not only as a problem *per se* in dynamical systems but also as its potential application in understanding real physical processes such as the ones described above.

In this paper we study numerically and analytically a version of the Burridge-Knopoff model. Our purpose is to scan the space of parameters in order to have better comprehension of the appearance of the solitary wave solutions reported by Schmittbuhl *et al.* [10]. We observe two kinds of transitions leading to different regimes depending on the values of certain groups of parameters. The first transition has already been reported in [9] and is obtained by varying the velocity scale of the friction law. The second transition we report is obtained when the rigidity of the chain of springs is varied. The sequence for increasing rigidity is from local periodic motions to chaotic and/or solitary wave motions and from there to

global periodic motion. For fixed rigidity, the transition from chaotic to solitary wave solutions has been described in Ref. [10]. Here we show that the proper control parameter is θ/l (see below) and not just θ as stated in Ref. [10].

The paper is organized as follows. In Sec. II we introduce the model and present the simulation results. In Sec. III we study the dynamics of a single free block and in Sec. IV we consider the motion of the system when a soliton is present. Finally, some conclusions are presented.

II. THE MODEL AND ITS NUMERICAL SOLUTION

The Burridge-Knopoff model consists of a set of N identical blocks of mass m connected with Hookean springs of constant k_c. Each block is moving in 1D and is connected with another spring of constant k_p to a pulling bar moving at constant velocity V. Finally, each block experiences a friction force which depends nonlinearly on the velocity of the blocks. The pulling bar may be moving in the direction of the chain or in the transverse direction as this leaves unaltered the resulting equations of motion. We find it more convenient for visualization of the macrodislocations to think in terms of the transverse geometry as depicted in the inset of Fig. 1(a).

The nontrivial element in the model is the friction law of force. It is postulated as a monotonically *decreasing* function of the velocity and this is the essential source of instability in the distribution of forces on the blocks. We select the following form for the friction force:

$$F(v) = -\frac{F_0}{1 + v/v_f}, \tag{1}$$

where v_f is a characteristic velocity for the friction (we follow the notation in Ref. [9]). It is also postulated that when a particle is at rest it remains at rest until the force exerted by all the springs connected with it exceeds the threshold friction F_0. For simplicity in the analytical results to be presented, only forward motions are allowed in this model (i.e., $v \geq 0$) [7]. In the numerical im-

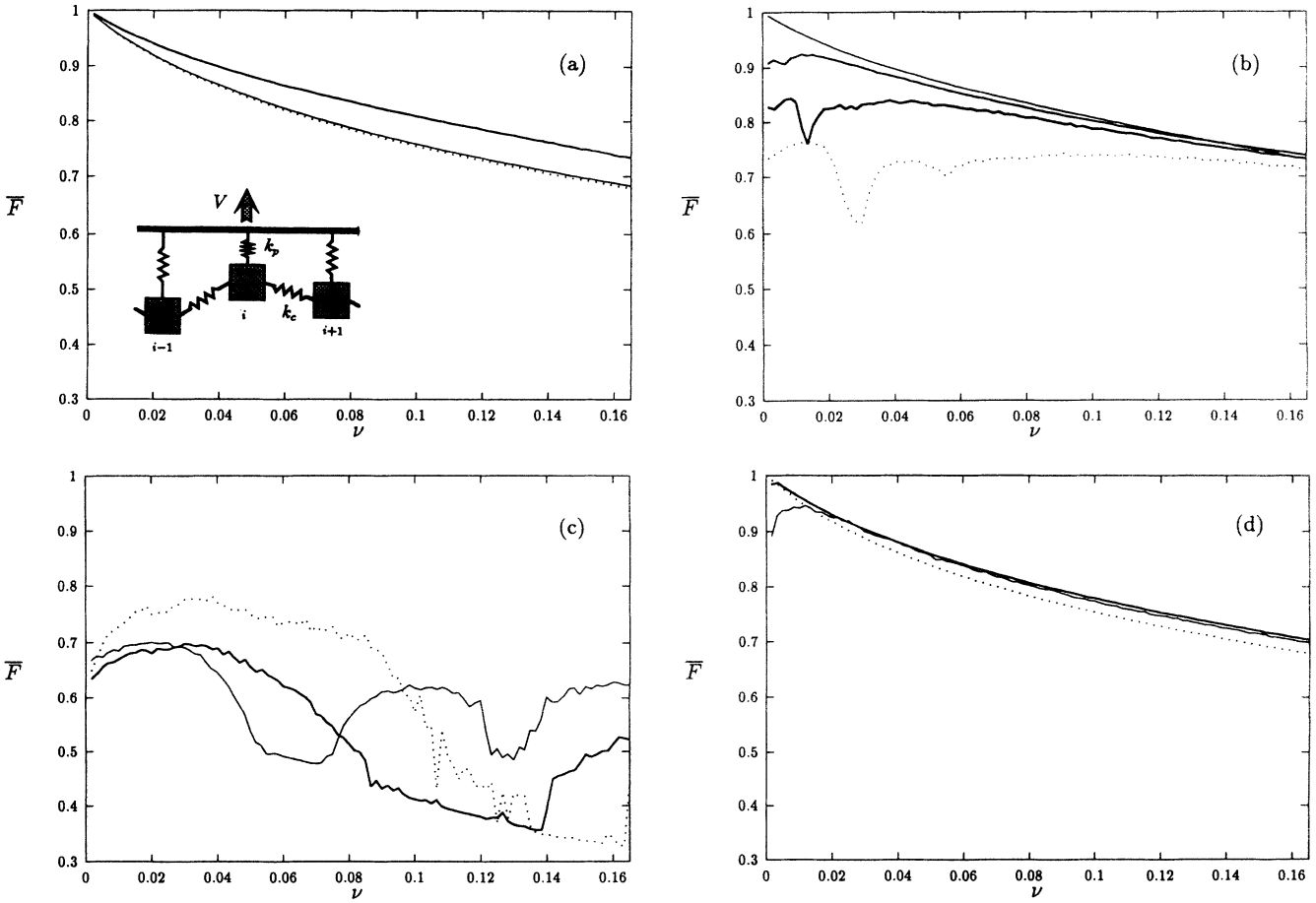

FIG. 1. The average friction force per particle $\overline{F}$ as a function of the pulling velocity ν for $\nu_f = 1$ and different values of l. (a) shows the curves for $l = 0$ (· · ·), $l = 0.1$ (——), and $l = 1$ (——). Inset: a schematic diagram of the Burridge-Knopoff model. (b) is for $l = 1$ (——), $l = 2$ (——), $l = 3$ (——), $l = 5$ (· · ·). (c) is for $l = 10$ (——), $l = 20$ (——), $l = 30$ (· · ·) and, (d) is for $l = 40$ (——), $l = 50$ (——), $l = 0 = \infty$ (· · ·).

plementation, this means that the blocks move forward until they reach a state of rest. At that point the velocity is maintained at zero until the force due to the springs overcomes the threshold F_0 of static friction allowing for forward motion again.

If $X_i(t)$ denotes the position of the ith block with respect to a laboratory reference frame, the equations of motion for the moving particles in the chain are

$$m\ddot{X}_i = k_p(R_0 + Vt - X_i) + k_c(X_{i+1} - 2X_i + X_{i-1}) + F(\dot{X}_i), \tag{2}$$

where R_0 is the position of the bar at the initial time. We will assume always periodic boundary conditions by identifying the particles 1 and $N+1$ (and the particles 0 and N).

By choosing the units of space and time as F_0/k_p and $\omega_p^{-1} \equiv (m/k_p)^{1/2}$, respectively, the equation of motion takes the dimensionless form

$$\ddot{x}_i = (r_0 + \nu t - x_i) + l^2(x_{i+1} - 2x_i + x_{i-1}) - \phi(\dot{x}_i/\nu_f), \tag{3}$$

where $x_i = X_i k_p/F_0$, $\tau = \omega_p t$, and the dot means differentiation with respect to τ. In addition,

$$\begin{aligned} \nu &\equiv \frac{k_p}{F_0\omega_p}V, \\ \nu_f &\equiv \frac{k_p}{F_0\omega_p}v_f, \\ l^2 &\equiv \frac{k_c}{k_p}, \\ \phi(x) &= \frac{1}{1+x}. \end{aligned} \tag{4}$$

In Ref. [6] the parameter $2\alpha = \nu_f^{-1}$ is used. The parameter l corresponds to the speed of sound of the harmonic chain. We have solved numerically Eqs. (3) for different values of the parameters ν, ν_f, l, N. As the parameter space is four dimensional, we expect to have a rich phenomenology. The first step in order to have some insight into the behavior of the system is to find a single magnitude which captures this behavior. As it is shown in Ref. [10], the average friction force per particle $\overline{F} \equiv \frac{1}{N}\sum_{i=1}^{N}\langle\phi(\dot{x}_i/\nu_f)\rangle$, where the angular brackets denote a time average, is a good magnitude for the following reason. For fixed ν_f, l, N the average friction force as a function of the pulling velocity ν presents some local minima precisely at the points where solitary waves exist [10]. This is because a macrodislocation is a very effective way of reducing friction in the system. Therefore the presence of minima in the curves of average friction force will indicate solitonic activity in the chain of blocks.

We solve the equations with a Runge-Kutta scheme with fixed time step. We have experimented with different time steps in order to select the appropriate one (large enough to have good computational efficiency and small enough to obtain reproducibility with even shorter time steps). Starting with a small spatial perturbation (of amplitude 0.001) and zero velocity we evolve the system during 500 units of time until it reaches a steady state where in a statistical sense the physical magnitudes do not show any temporal drift.

From then on we compute the average friction force per particle from a trajectory 20.000 units of time long. Initially we fix the number of blocks to $N = 120$ and select two values for $\nu_f = 0.2$ and 1 (corresponding to $\alpha = 2.5, 0.5$). The results for $\nu_f = 1$ are presented in Fig. 1, where the average friction force is plotted as a function of the dimensionless pulling velocity ν for different values of the sound speed l. We observe in Fig. 1(a) that the average friction force for a single free block ($l = 0$) represents a lower bound of the curves in that figure. As l increases, the average friction increases, but the overall pattern is a monotonically decreasing function of the pulling velocity. At a value around $l = 1$ a transition occurs as shown in Fig. 1(b). This transition is characterized by the appearance of local minima and by a global reduction of the average friction. By further increasing l new minima appear in the curves, as can be observed in the curve for $l = 10$ in Fig. 1(c). Finally, when l reaches a value around 40, the minima disappear as shown in Fig. 1(d). We have also plotted the curve $l = 0$ in Fig. 1(d) for comparison, because it coincides with the curve $l = \infty$ when all blocks are moving as a rigid solid.

The limits $l = 0$, $l = \infty$ correspond to the single block motion and rigid motion, respectively, and the motion of the blocks will be essentially the same in both limits, i.e., periodic motion. The transition as l is increased is therefore a three step transition, from free motion to cooperative motion and from cooperative motion to rigid motion. The visual inspection of the trace of the motion of the chain as l is increased is very revealing [see Figs. 2(a)–2(e)]. For small l the motion of each individual block is periodic, but the small coupling with the rest of the chain renders an alternating pattern as depicted in Fig. 2(a). We have checked that the periodicity of each block translates into a periodic pattern for the velocity of the center of mass. For large l the motion is also periodic, as shown in Fig. 2(e). For intermediate values of l we observe that there exists a certain amount of solitonic activity, where small fractures propagate in both directions. Quite remarkably, for $l = 2$ [Fig. 2(c)] we observe a qualitatively distinct behavior where the solitons run through the whole system. This coincides with the appearance of a first minimum in the curve of the average friction force. For $l = 10$ [Fig. 2(d)] we observe solitons which give approximately two turns to the chain before decaying. By increasing the pulling speed [Fig. 2(f)] the soliton becomes stable at $\nu = 0.068$, where the first minimum of the average friction force occurs for these N, ν_f, l. We have also confirmed the observations by Schmittbuhl, Vilotte, and Roux [10] concerning the existence of two solitary waves for the second valley (whenever it exists), three for the third, etc.

The curves of average friction force for $\nu_f = 0.2$ have a behavior similar to the ones with $\nu_f = 1$, as it is shown in Fig. 3. We observe a transition for $l \sim 1$ from mono-

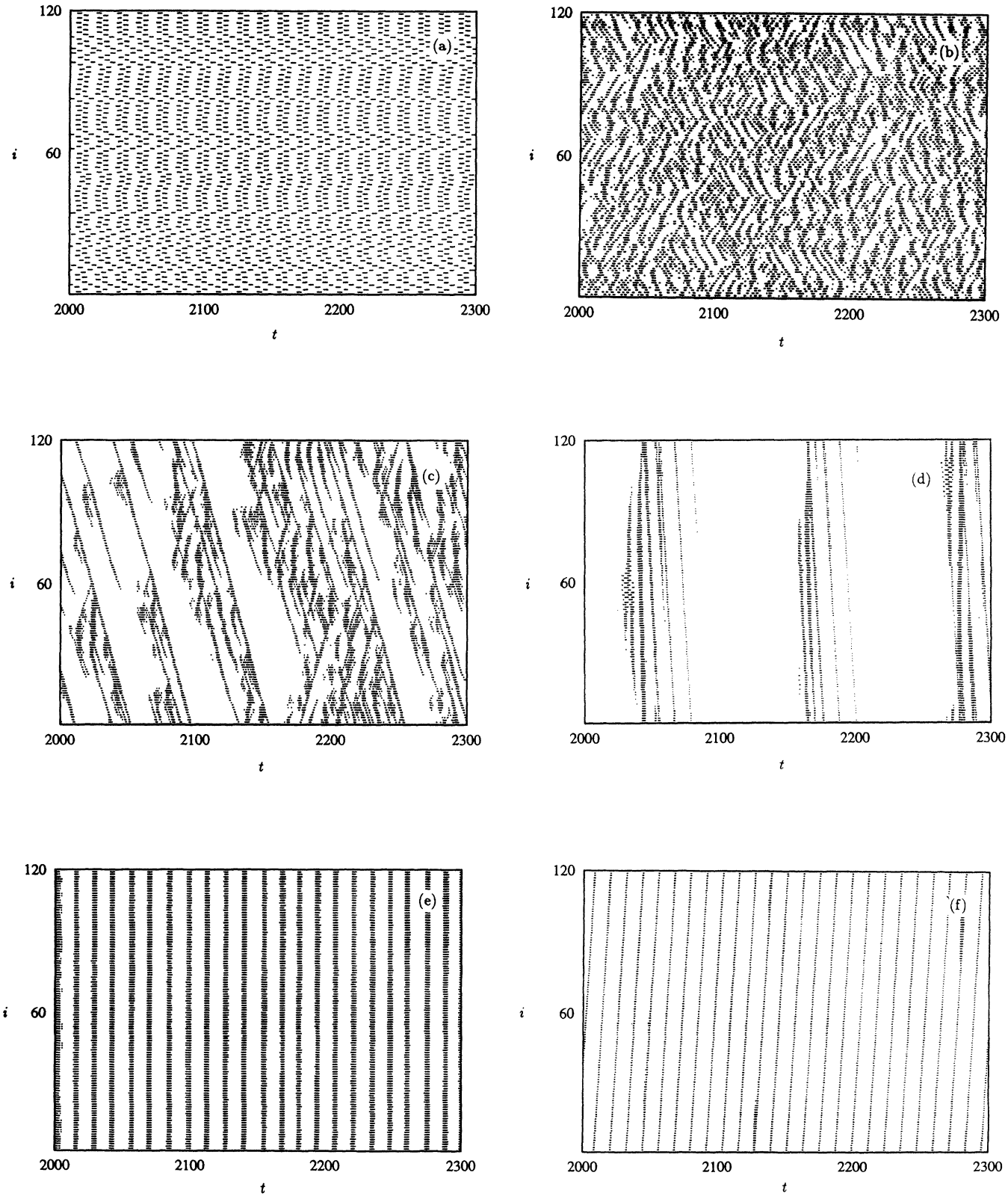

FIG. 2. Image of the moving blocks for $N = 120, \nu_f = 1, \nu = 0.01$, and different values for the speed of sound l. A black dot in the horizontal line corresponding to particle i denotes that this particle is moving at time t. (a) $l = 0.1$, (b) $l = 1$, (c) $l = 2$, (d) $l = 10$, (e) $l = 60$. Also shown in (f) is the soliton that arises for $l = 10$ and $\nu = 0.068$. Finally, (g) the image for $N = 120, \nu_f = 0.2, \nu = 0.01, l = 1$. The images for (b) and (g) differ only in the value of ν_f.

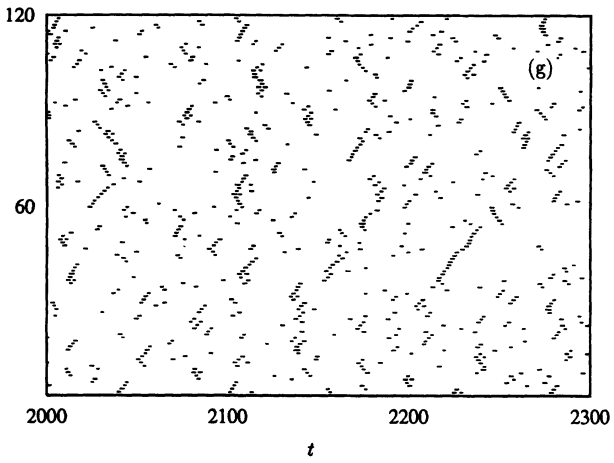

FIG. 2 *(Continued).*

tonically decreasing curves to curves with minima which tend to disappear as $l \geq 60$. However, a difference between $\nu_f = 1$ and $\nu_f = 0.2$ must be noted. For $\nu_f = 1$ and small l the average friction goes to 1 as ν goes to 0, whereas for $\nu_f = 0.2$ this is not so. This suggests that a transition with ν_f is in order [9]. By comparing the pictures of the system in Fig. 2(b) and Fig. 2(g) we observe strikingly different states of motion. In the next section we trace back the different global behavior for $\nu_f = 0.2$ and $\nu_f = 1$ to what is happening in the case of a single free block.

Schmittbuhl *et al.* show that, for fixed l, the average friction force depends on N and ν through the parameter $\theta \equiv N\nu$. We have performed another set of simulations for a number of particles $N = 80$. In Fig. 4 we plot the average friction force as a function of ν and θ for $\nu_f = 0.2$ and $l = 1, 10$. We observe that the "solitonic" curves (those exhibiting minima) have their minimum for the same value of θ but the nonsolitonic curves are not functions of N and ν through θ.

When l is varying, we have observed that the relevant parameter for the location of the minima is θ/l. This can be seen in Fig. 5, where we represent the average friction force as a function of $N\nu/l$ for $\nu_f = 1$. We observe that the location of the first minimum is at the same value of this parameter, meaning that the solitons appear at a given value of this parameter. We also observe that the second minimum appears at a pulling velocity two times

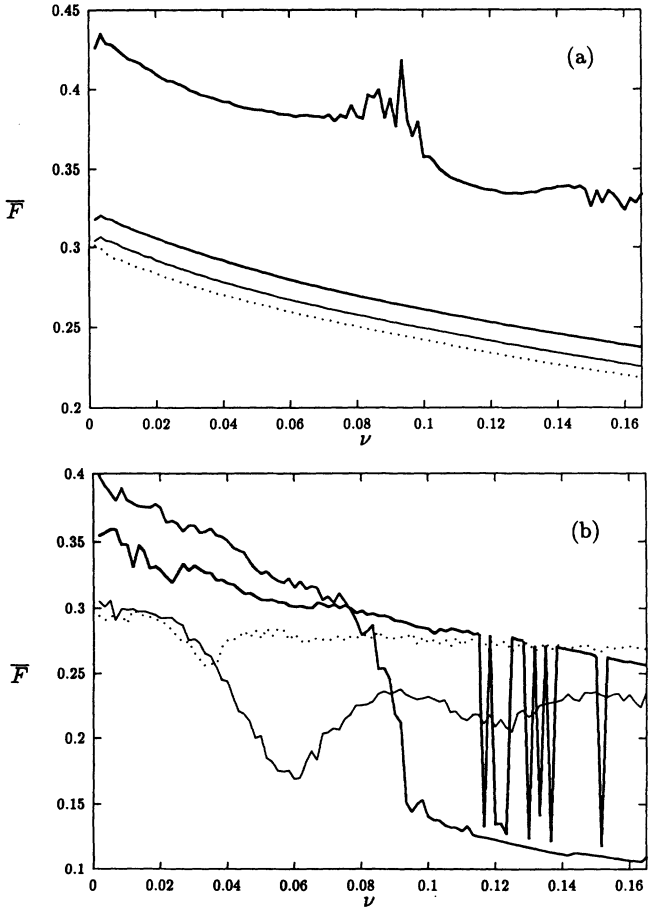

FIG. 3. The average friction force per particle $\overline{F}$ as a function of the pulling velocity ν for $\nu_f = 0.2$ and different values of l. In (a) $l = 0.1$ (· · ·), $l = 0.2$ (——), $l = 0.3$ (——), $l = 1$ (——), and in (b) $l = 5$ (· · ·), $l = 10$ (——), $l = 40$ (——), $l = 60$ (——).

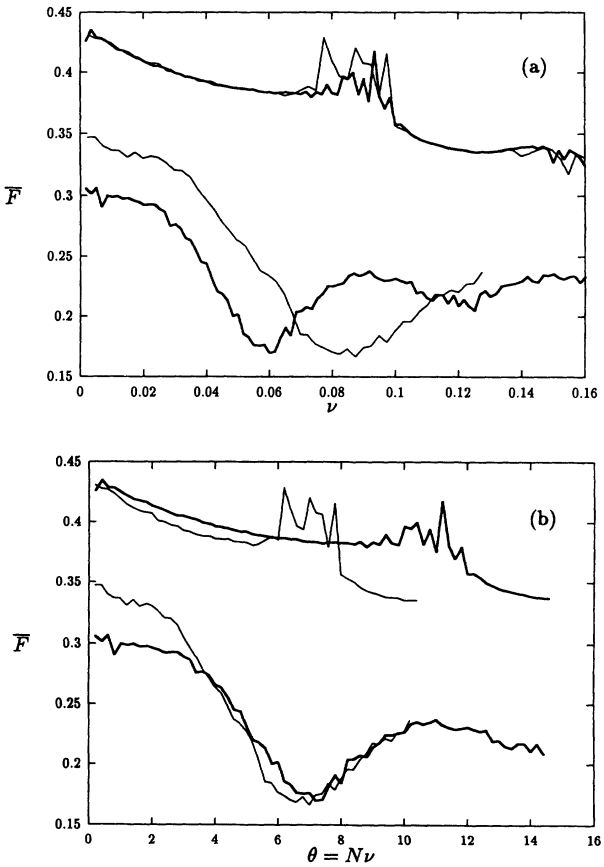

FIG. 4. Scaling of the curves of friction for $\nu_f = 0.2$ and different numbers of particles. Curves (——) are for $N = 80$ and curves (——) are for $N = 120$. The upper curves are for $l = 1$, the lower for $l = 10$. In (a) the average friction force is represented in front of ν whereas in (b) it is represented in front of $\theta \equiv N\nu$.

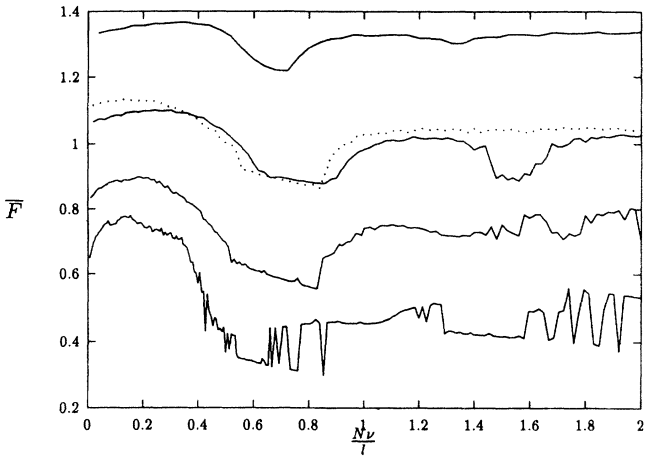

FIG. 5. Scaling with $N\nu/l$ of the solitonic curves of average friction. The average friction for $\nu_f = 1$ is plotted against $N\nu/l$ for $N = 120$ (solid lines) for $l = 5, 10, 20, 30$ (in descending order) and $N = 80$ (dotted line) for $l = 10$. The curves have been vertically displaced for a better display, compare with Fig. 1(c). The location of the first minimum is the same for all the curves.

larger than the corresponding one for the first minimum. In this figure it is also apparent that the second minimum for $N = 120, \nu_f = 1.0, l = 10$ corresponding to two solitary waves is not present for $N = 80, \nu_f = 1.0, l = 10$.

In the next sections, we will obtain some analytical results which shed some light on the nature of the two transitions observed when the parameters ν_f and l are varied.

III. EQUATION FOR A SINGLE FREE BLOCK

We have noted that the curves of average friction for $\nu_f = 0.2$ and $\nu_f = 1$ have different global behavior. For small l, the curves with $\nu_f = 1$ go to 1 as ν goes to zero, whereas the curves with $\nu_f = 0.2$ do not go to 1. In order to understand what is happening it is useful to look at the limiting case where $l = 0$. The case $l = 0$ corresponds to a single free block with equation of motion

$$\ddot{x}(\tau) = r_0 + \nu t - x(\tau) - \phi(\dot{x}/\nu_f). \tag{5}$$

This equation has periodic solutions. If the initial conditions are $r_0 = 1$, $x(0) = 0$, and $\dot{x}(0) = 0$, then the particle is initially on the verge of instability. In this case, the tension of the spring equates the threshold of static friction which in the dimensionless units is 1. The particle starts moving at time $\tau = 0$ until the velocity vanishes at time τ_m after traveling a distance $x_m = x(\tau_m)$. Then it remains stuck until time T where the tension of the spring again overcomes the static friction, that is, $1 + \nu T - x_m = 1$. From then on the motion repeats periodically. The distance x_m will be in general a parametric function of ν, ν_f, i.e.,

$$x_m = g(\nu, \nu_f). \tag{6}$$

For later convenience, in Fig. 6 we plot the form of the

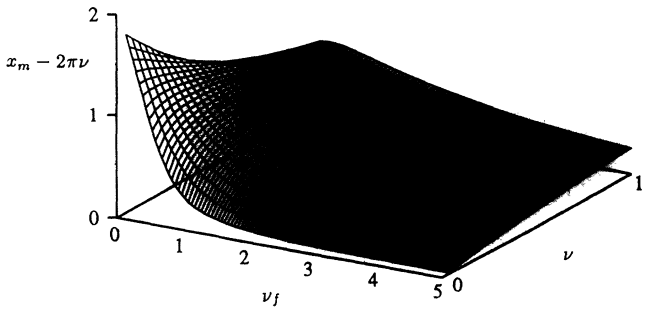

FIG. 6. The function $g(\nu, \nu_f) - 2\pi\nu$. The maximum displacement x_m for a single block as a function of ν and ν_f is given by $x_m = g(\nu, \nu_f)$.

function $g(\nu, \nu_f) - 2\pi\nu$ which has been computed numerically. Equation (5) can be solved analytically in two limiting cases, when $\nu_f = 0$ and when $\nu_f = \infty$. Let us discuss the $\nu_f = 0$ case first, when the equation of motion becomes $\ddot{x}(\tau) = 1 + \nu t - x(\tau)$. The solution with the above mentioned initial conditions is $x(\tau) = [1 - \cos(\tau)] + \nu[\tau - \sin(\tau)]$. It is possible to find x_m, t_m by solving $\dot{x}(\tau) = 0$ (i.e., $\sin(\tau) + \nu[1 - \cos(\tau)] = 0$) with the result $\cos(\tau_m) = (\nu^2 \pm 1)/(\nu^2 + 1)$. When $\nu = 0$ the nontrivial solution is $\cos(\tau_m) = -1$, implying

$$\begin{aligned} \tau_m &= \pi, \\ x_m &= 2. \end{aligned} \tag{7}$$

In the case $\nu_f \sim \infty$ the equation of motion takes the form $\ddot{x}(\tau) = \nu\tau - x(\tau)$ with solution $x(\tau) = \nu[\tau - \sin(\tau)]$. In this case, for all ν we have

$$\begin{aligned} \tau_m &= 2\pi, \\ x_m &= 2\pi\nu. \end{aligned} \tag{8}$$

In this case the period $T = x_m/\nu$ is equal to τ_m and the particle never stops. The asymptotic results in Eqs. (7) and (8) can be appreciated in Fig. 6.

Equations (7) and (8) suggest that for small values of ν there exists a transition as ν_f goes from zero to infinity because for small values of ν_f the jump in position of the particle is large (of the order of 2) whereas for large ν_f this jump is very small ($2\pi\nu$). The transition can be described as a transition from a stick-slip motion for $\nu_f = 0$ to a quasicontinuous motion for $\nu_f = \infty$. The question is, of course, whether this transition is sharp. In Fig. 6 we observe that the transition smooths when ν grows while for small ν there is a tendency towards a sharp transition. The smaller ν depicted in Fig. 6 is $\nu = 0.033$. In Fig. 7 we present the maximum displacement x_m as a function of ν_f for smaller values of ν, i.e., $\nu = 10^{-4}, 10^{-3}, 5 \times 10^{-3}, 10^{-2}$. As $\nu \to 0$, we observe the tendency towards a sharp transition at $\nu_f = 0.5$ or, equivalently, $\alpha = 1$. This transition is also reflected in the average friction force $\overline{F}$ affecting the particle, as shown in Fig. 8. We observe that when $\nu_f > 0.5$ the average friction force reaches a constant plateau value $\overline{F} = 1$. In the limit

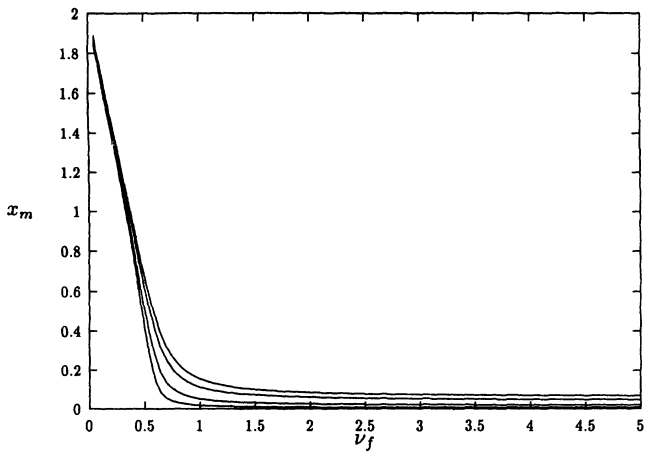

FIG. 7. The maximum displacement x_m for a single block as a function of ν_f and for small ν. The upper curve is for $\nu = 10^{-2}$ and in descending order the curves for $\nu = 5 \times 10^{-3}, 10^{-3}, 10^{-4}$ follow.

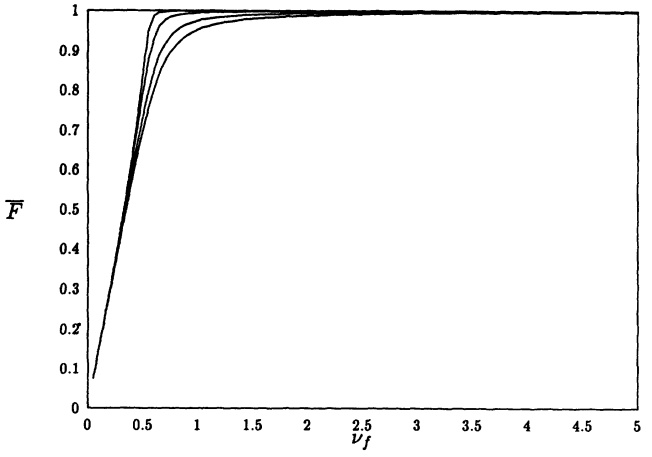

FIG. 8. The average friction force for a single block as a function of ν_f for small ν. The lower curve is for $\nu = 10^{-2}$ and in ascending order the curves are for $\nu = 5 \times 10^{-3}, 10^{-3}, 10^{-4}$.

$\nu_f \to \infty$ the average friction force is 1 because

$$\overline{F} = \lim_{T\to\infty} \frac{1}{T} \int_0^T [1 + \nu\tau - x(\tau)] d\tau \tag{9}$$

and $x(\tau) = \nu[\tau - \sin(\tau)]$. We therefore conclude that in the limit $\nu \to 0$ there is a discontinuous transition as the parameter ν_f is varied. For values of ν_f larger than 0.5 the motion is quasicontinuous while for ν_f smaller than 0.5 the motion is of the stick-slip type. In terms of the average friction force the transition implies that for the quasicontinuous motion $\overline{F} = 1$ whereas for the stick-slip motion the friction is smaller.

The presence of a transition for a single block when $\nu \sim 0$ and ν_f is varied is also relevant for the case of interacting blocks. The idea is that $l = 0$ and $l = \infty$ are the limiting cases for the curves of friction corresponding to a given ν_f. Therefore all friction curves for a given ν_f will exhibit the same trends as the limiting friction curves, which correspond to the single block case. In addition, the actual motion of the interacting chain also reveals a qualitatively distinct behavior of the blocks for different ν_f as can be appreciated in Figs. 2(b) and 2(g). In Fig. 2(b) the particles move in a more continuous way than in Fig. 2(g).

IV. PROPAGATIVE SLIPPING MODES

The motion of a block when the chain is moving through a solitary wave is very similar to the motion of a free block, except for the reduced mass to be assigned to it. The motion has an intrinsic period determined by the threshold condition. In order to comply with the periodic boundary conditions it is a necessary condition that the intrinsic period coincides with the period of revolution of the solitary wave, and this imposes a restriction on the values of the parameters that allow a solitary wave to exist in the chain. Finally, the dissipative condition requiring that the rate of input of energy and the dissipation should exactly balance when a stable soliton is present fixes completely the value of the pulling velocity at which there exists a soliton once the rest of the parameters are fixed. Let us study this in some detail.

In order to investigate the solitary wave solutions, it is convenient to take the continuum limit of Eq. (2). Following Carlson and Langer [6] we introduce variables $s \equiv ia$ and $\zeta = la$, where a is the (small) equilibrium distance between blocks, and the equation of motion (3) becomes

$$\ddot{x}(s,\tau) = r_0 + \nu\tau - x(s,\tau) + \zeta^2 x''(s,\tau) - \phi[\dot{x}(s,\tau)/\nu_f], \tag{10}$$

where the double prime denotes second derivatives with respect to s.

In the following we will assume that the chain sustains a solitary wave of the form

$$\begin{aligned} x(s,\tau) &= f(\tau - s/\beta) + r_0 + \nu\tau, \\ \dot{x}(s,\tau) &= f'(\tau - s/\beta) + \nu. \end{aligned} \tag{11}$$

Here, β is the unknown velocity of the wave. By substitution of this solution into (10) we obtain the following equation of motion for the particle located at $s = 0$:

$$\mu\ddot{x}(0,\tau) = r_0 + \nu\tau - x(0,\tau) - \phi[\dot{x}(0,\tau)/\nu_f], \tag{12}$$

which is similar to the equation for a single block (5) except for the reduced mass $\mu \equiv 1 - \zeta^2/\beta^2$. This means that the motion of a particular block when the chain sustains a stable soliton is equivalent to the motion of a single block of reduced mass. We select origins in such a way that at $\tau = 0$ the particle at $s = 0$ is on the verge of stability. In this case, $x(0,0) = 0$, $\dot{x}(0,0) = 0$, and, furthermore, $\ddot{x}(0,0) = 0$. Let us locate now the position

r_0 of the pulling bar at the initial time. Because the particle at $s = 0$ is on the verge of stability we have

$$r_0 + \zeta^2 x''(0,0) = 1. \tag{13}$$

This means that the force (r_0) exerted on the block at $s = 0$ by the pulling spring plus the force $[\zeta^2 x''(0,0)]$ due to the neighbor particles should equate the static friction threshold (which is 1). If the chain moves with a soliton, then $\ddot{x}(0,0) = 0$ implies $x''(0,0) = 0$ and therefore $r_0 = 1$. The condition $x''(0,0) = 0$ means that at the initial time the neighbor springs are equally stretched in opposite directions and, therefore, the force exerted on the particle is due to the pulling spring and the friction only.

In the same way as for a single block, the particle at $s = 0$ will move a distance x_m^s until it becomes stuck at time τ_m^s because the velocity vanishes at that time. It then remains stuck until time T^s when the springs' force overcomes the friction force again and the motion repeats periodically. The intrinsic period T^s of the particle at $s = 0$ is given by the threshold condition $r_0 + \nu T^s - x_m^s = 1$, i.e., $T^s = x_m^s/\nu$.

It is a *condition* to be imposed that this time T^s should coincide with the period of revolution of the soliton, which is L/β, where $L \equiv Na$ is the length of the chain. This condition, in turn, will ensure that the velocity of the center of mass of the chain equals the pulling velocity.

It is not necessary to solve again Eq. (12) in order to find x_m^s, τ_m^s as a function of the parameters ν, ν_f, and ζ. By defining a stretched time variable $\tilde{\tau} = \tau/\epsilon$ where $\epsilon \equiv \mu^{1/2}$ $(0 \leq \epsilon \leq 1)$ we can write (12) in exactly the same form as (5) with the parameters $\tilde{\nu} \equiv \epsilon\nu, \tilde{\nu}_f \equiv \epsilon\nu_f$. Therefore we have

$$x_m^s = g(\epsilon\nu, \epsilon\nu_f), \tag{14}$$

where the function g is the same as in Eq. (6). The condition that the intrinsic period T^s should be equal to the period of revolution of the soliton (or a submultiple of it) implies

$$\frac{x_m^s}{\nu} = \frac{g(\epsilon\nu, \epsilon\nu_f)}{\nu} = \frac{L}{n\beta}, \tag{15}$$

where n is an integer. For $n = 2$ we have two identical solitons moving in the same direction at the same speed and separated by a distance $L/2$ from each other, etc. By using $\epsilon = (1 - \frac{\zeta^2}{\beta^2})^{1/2}$ this equation takes the form

$$G(\epsilon; \nu, \nu_f) \equiv \frac{1}{(1-\epsilon^2)^{1/2}} g(\epsilon\nu, \epsilon\nu_f) = \frac{\nu L}{n\zeta}. \tag{16}$$

This is an implicit equation for ϵ which, in turn, allows us to obtain the velocity β of the solitary wave.

The most important feature of $G(\epsilon; \nu, \nu_f)$ is that it is a function of ϵ bounded from below by a certain value G_0, for all ν, ν_f. One can appreciate this property in the graph of $g(\nu, \nu_f)$ in Fig. 6. By fixing ν, ν_f, the function $g(\epsilon\nu, \epsilon\nu_f)$ goes from 2 to $g(\nu, \nu_f)$ as ϵ goes from 0 to 1, whereas the factor $\frac{1}{(1-\epsilon^2)^{1/2}}$ diverges at $\epsilon = 1$. As a consequence, Eq. (16) will have a solution only if

$$\frac{\nu L}{n\zeta} = \frac{\nu N}{nl} \geq G_0. \tag{17}$$

This is a necessary condition for the system having n solitons.

There exists another condition that the solitary wave configuration has to satisfy, which is a dissipative condition. The dissipative condition states that as the soliton evolves steadily, the rate of input of energy into the system must equate the rate of energy dissipated [10]. It might be convenient at this point to recall some aspects of the dissipation of energy in this system. In the discrete version of the chain, the total energy of the system is given by the kinetic energy plus the potential energy stored in the pulling spring and the connecting springs. In reduced units,

$$H = \sum_{i=1}^{N} \left(\frac{v_i^2}{2} + \frac{1}{2}(1 + \nu\tau - x_i)^2 + \frac{l^2}{2}(x_i - x_{i-1})^2 \right). \tag{18}$$

We may use the equations of motion (3) in order to compute the time derivative of the energy with the result

$$\dot{H} = -\sum_{i=1}^{N} \phi(v_i/\nu_f) v_i + \sum_{i=1}^{N} \nu(1 + \nu\tau - x_i). \tag{19}$$

In obtaining this result, the periodicity of the chain has been used (i.e., $x_0 = x_N$ and $x_{N+1} = x_1$). The first term in the right hand side of (19) accounts for the rate of dissipation due to the frictional forces whereas the second is the rate of input of energy due to the pulling springs. In the continuum limit we have

$$\begin{aligned} \dot{H} &= -\int_0^L \phi[\dot{x}(s,\tau)/\nu_f]\dot{x}(s,\tau)ds \\ &\quad +\nu \int_0^L [1 + \nu\tau - x(s,\tau)]ds \\ &\equiv -D + I. \end{aligned} \tag{20}$$

If the system is moving with a solitary wave, then $\dot{H} = 0$ and the dissipation exactly balances the input of energy, i.e., $D = I$. We could insert in (20) the solitary wave solution which will now be a parametric function of ν, ν_f, ζ, L. The integral over s eliminates the time and position dependence and we are left with an implicit condition to be satisfied by the four parameters. By fixing ν_f, ζ, L, for example, we obtain a unique value of ν which allows the solitary wave to comply with the dissipative condition. This explains why a stable soliton is obtained only for a particular value of ν, once the rest of the parameters are fixed.

It is interesting to check that the predictions of Eq. (17) are entirely consistent with our observations of the friction curves. Perhaps the most important consequence of (17) is that the first valley corresponding to one soliton will appear for a constant value of $\nu N/l = \theta/l$, as is seen in Fig. 5. The second valley corresponding to two solitons $n = 2$ appears for a value of the group $\nu N/l$ two times

larger than for the first valley. As l is increased, we have observed that the valleys disappear suddenly [see Figs. 1(c) and 1(d)]. Finally, as N is decreased, some of the valleys disappear, as in the case of the second valley for $N = 80$ in Fig. 5.

V. CONCLUDING REMARKS

We have investigated the influence of the parameters ν_f and l in the motion of the blocks in a version of the Burridge-Knopoff model. We have observed that as the velocity scale ν_f of the friction force is decreased, there is a transition from a quasicontinuous motion to a stick-slip motion of the blocks. This implies that the average friction also experiences a transition, from the value 1 for quasicontinuous motion to values smaller than 1 for the stick-slip motion. The possibility of this transition has been suggested by Carlson and Langer after their observation that the scaling of the distribution of magnitudes of the slipping events changes as the parameter $\alpha = 1/2\nu_f$ approaches 1 [6]. They hypothesized that if there was such a transition it could depend on the pulling speed ν. We have seen that the transition exists for a single block and it is very sharp in the limit of small pulling speeds. The change of behavior as ν_f is varied has also been studied by de Sousa Vieira *et al.* [9] and they also observe this transition but at a value of $\nu_f = 1$, i.e., $\alpha = 0.5$, instead of the value $\alpha = 1$ reported by Carlson and Langer. It seems like a factor of 2 is missing somewhere. As our law of friction is not exactly the same as those in Refs. [6,9] (in the sense that we do not allow backward motions), we cannot elucidate the location of the source of the discrepancy.

When the parameter l is varied, we have observed that there is an interval of solitonic activity between two values of l_{free} and l_{rigid}. When $l < l_{\text{free}}$ or $l > l_{\text{rigid}}$ the blocks in the chain move periodically whereas for $l_{\text{free}} < l < l_{\text{rigid}}$ the blocks exhibit more complex behavior. This behavior is characterized by the appearance of propagating fractures at a speed slightly larger than the speed of sound. It is within this range of values of l where chaotic motions are observed for small values of the pulling velocity and solitary waves for larger values of ν. The solitonic activity is reflected in the form of the average friction force. In the solitonic interval $l_{\text{free}} < l < l_{\text{rigid}}$ the curves present some minima and globally the friction is reduced. The minima occur for a given value of the group $N\nu/l$. Therefore when representing the average friction force in front of this group we obtain an approximate scaling of the curves. This scaling is not obtained for the nonsolitonic curves, when the motion of the blocks is periodic.

We have obtained a necessary condition for the existence of a solitary wave. This condition states that the group $\nu N/l$ should be larger than a certain value G_0 and this allows us to understand many of the trends of the average friction curves. In particular, it is obtained that when l increases the solitary wave mode of motion disappears. This has been observed in the experiments by Rubio and Galeano [11] where by increasing the rigidity of the gel they observe that the motion is no longer through propagating localized slipping regions but through global relaxation of the gel as a whole in a quasiperiodic way.

ACKNOWLEDGMENTS

I am very much indebted to M.A. Rubio for his comments and suggestions during the elaboration of this work. I also appreciate the comments by R. Ball and J.-P. Bouchaud and, in an early stage of this work by J. Schmittbuhl. This work has been supported by a grant in the Human Capital and Mobility Programme from the E.E.C. and DGICYT Project No. PB91-222.

[1] P. Bak, C. Tang, and K. Wiesenfeld, Phys. Rev. A **38**, 364 (1988).
[2] H. Takayasu and H. Inaoka, Phys. Rev. Lett. **68**, 966 (1992).
[3] R.L. Leheny and S.R. Nagel, Phys. Rev. Lett. **71**, 1470 (1993).
[4] K. Chen, P. Bak, and S.P. Obukhov, Phys. Rev. A **43**, 625 (1991); Z. Olami, H.J.S. Feder, and K. Christensen, Phys. Rev. Lett. **68**, 1244 (1992); Z. Olami and K. Christensen, Phys. Rev. A **46**, 1720 (1992); H. Nakanishi, *ibid.* **46**, 4689 (1992).
[5] R. Burridge and L. Knopoff, Bull. Seismol. Soc. Am. **57**, 341 (1967).
[6] J.M. Carlson and J.S. Langer, Phys. Rev. A **40**, 6470 (1989).
[7] J.M. Carlson, J.S. Langer, B.E. Shaw, and C. Tang, Phys. Rev. A **44**, 884 (1991).
[8] J.S. Langer and C. Tang, Phys. Rev. Lett. **67**, 1043 (1991).
[9] M. de Sousa Vieira, G.L. Vasconcelos, and S. R. Nagel, Phys. Rev. E **47**, 2221 (1993).
[10] J. Schmittbuhl, J.-P. Vilotte, and S. Roux, Europhys. Lett. **21**, 375 (1993).
[11] M.A. Rubio and J. Galeano, Phys. Rev. E (to be published).
[12] R.G. Larson, Rheol. Acta **31**, 213 (1992).
[13] N. El Kissi and J.M. Piau, J. Non-Newt. Fluid Mech. **37**, 55 (1990).
[14] P. Español (unpublished).

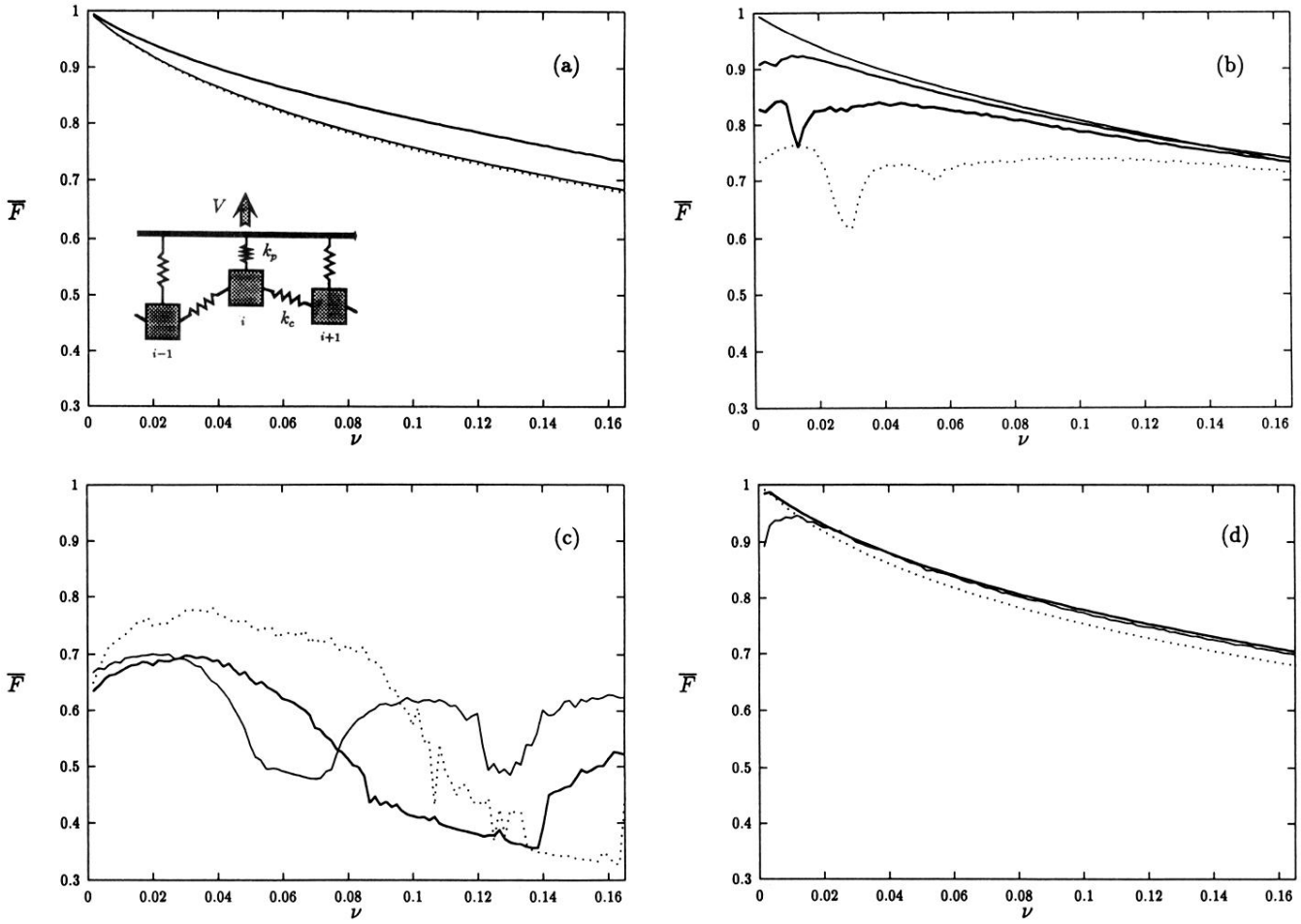

FIG. 1. The average friction force per particle $\overline{F}$ as a function of the pulling velocity ν for $\nu_f = 1$ and different values of l. (a) shows the curves for $l = 0$ (· · ·), $l = 0.1$ (——), and $l = 1$ (——). Inset: a schematic diagram of the Burridge-Knopoff model. (b) is for $l = 1$ (——), $l = 2$ (——), $l = 3$ (——), $l = 5$ (· · ·). (c) is for $l = 10$ (——), $l = 20$ (——), $l = 30$ (· · ·) and, (d) is for $l = 40$ (——), $l = 50$ (——), $l = 0 = \infty$ (· · ·).

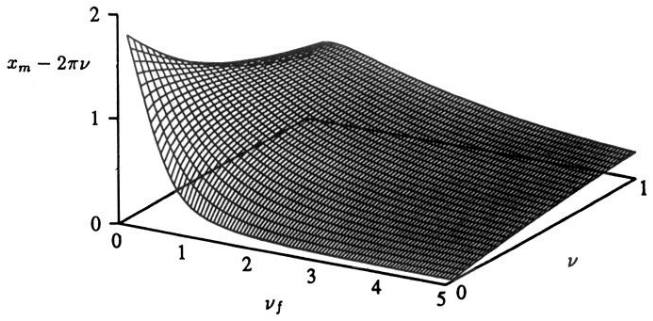

FIG. 6. The function $g(\nu, \nu_f) - 2\pi\nu$. The maximum displacement x_m for a single block as a function of ν and ν_f is given by $x_m = g(\nu, \nu_f)$.